







Adaptations in equine axial movement and muscle activity occur during induced fore- and hindlimb lameness: A kinematic and electromyographic evaluation during in-hand trot

Tijn J. P. Spoormakers¹  | Lindsay St. George²  | Ineke H. Smit¹ | Sarah Jane Hobbs²  | Harold Brommer¹ | Hilary M. Clayton³  | Serge H. Roy⁴ | James Richards⁵  | Filipe Manuel Serra Bragança¹ 

¹Department of Clinical Sciences, Faculty of Veterinary Medicine, Utrecht University, Utrecht, The Netherlands

²Research Centre for Applied Sport, Physical Activity and Performance, University of Central Lancashire, Preston, UK

³Department of Large Animal Clinical Sciences, College of Veterinary Medicine, Michigan State University, East Lansing, Michigan, USA

⁴Delsys/Altec Inc., Natick, Massachusetts, USA

⁵Allied Health Research Unit, University of Central Lancashire, Preston, UK

Correspondence

Tijn J.P. Spoormakers, Department of Clinical Sciences, Faculty of Veterinary Medicine, Utrecht University, Utrecht, The Netherlands.
Email: tjpspoormakers@gmail.com

Funding information

British Society of Animal Science (BSAS) 2018 Steve Bishop Early Career Award, Grant/Award Number: BSAS 2018; Morris Animal Foundation, Grant/Award Number: D21EQ-406

Abstract

Background: The inter-relationship between equine thoracolumbar motion and muscle activation during normal locomotion and lameness is poorly understood.

Objective: To compare thoracolumbar and pelvic kinematics and longissimus dorsi (longissimus) activity of trotting horses between baseline and induced forelimb (iFL) and hindlimb (iHL) lameness.

Study design: Controlled experimental cross-over study.

Methods: Three-dimensional kinematic data from the thoracolumbar vertebrae and pelvis, and bilateral surface electromyography (sEMG) data from longissimus at T14 and L1, were collected synchronously from clinically nonlame horses ($n = 8$) trotting overground during a baseline evaluation, and during iFL and iHL conditions (2–3/5 AAEP), induced on separate days using a lameness model (modified horseshoe). Motion asymmetry parameters, maximal thoracolumbar flexion/extension and lateral bending angles, and pelvis range of motion (ROM) were calculated from kinematic data. Normalised average rectified value (ARV) and muscle activation onset, offset and activity duration were calculated from sEMG signals. Mixed model analysis and statistical parametric mapping compared discrete and continuous variables between conditions ($\alpha = 0.05$).

Results: Asymmetry parameters reflected the degree of iFL and iHL. Maximal thoracolumbar flexion and pelvis pitch ROM increased significantly following iFL and iHL. During iHL, peak lateral bending increased towards the nonlame side (NLS) and decreased towards the lame side (LS). Longissimus ARV significantly increased bilaterally at T14 and L1 for iHL, but only at LS L1 for iFL. Longissimus activation was significantly delayed on the NLS and precipitated on the LS during iHL, but these clear phasic shifts were not observed in iFL.

Main limitations: Findings should be confirmed in clinical cases.

Conclusions: Distinctive, significant adaptations in thoracolumbar and pelvic motion and underlying longissimus activity occur during iFL and iHL and are detectable using

combined motion capture and sEMG. For iFL, these adaptations occur primarily in a cranio-caudal direction, whereas for iHL, lateral bending and axial rotation are also involved.

KEYWORDS

gait analysis, horse, longissimus dorsi, sEMG, thoracolumbar, trot

1 | INTRODUCTION

Lameness and back pain are common clinical issues in horses that are often interrelated; lame horses can exhibit adaptive thoracolumbar movement and horses with back pain can show clinical signs of forelimb (FL) and/or hindlimb (HL) lameness.¹ Lameness is one of the main reasons for veterinary consultation,² and the prevalence of back problems has been reported to be as high as 94% in ridden horses.³ Despite this, the aetiology and clinical manifestation of equine back pain and the inter-relationship with FL and/or HL lameness, remain poorly understood, creating a diagnostic challenge.^{4,5}

Quantitative equine gait analysis has been applied to measure axial motion in nonlame horses^{6–9} and to quantify adaptive changes in axial motion in horses with induced lameness or back pain^{10–13} during treadmill locomotion. Increased thoracolumbar range of motion (ROM) was observed in horses with induced unilateral back pain¹² and FL lameness,¹⁰ but not during induced unilateral HL lameness.¹¹ These studies have advanced our understanding of adaptive axial movement associated with pain avoidance during treadmill locomotion, but clinical observations during overground locomotion indicate decreased thoracolumbar ROM during FL and/or HL lameness, which contradicts published findings.^{11,12} Furthermore, the underlying neuromuscular mechanisms that ultimately facilitate these movement adaptations are poorly understood and have not been quantified during standardised lameness conditions.

Surface electromyography (sEMG) offers a solution to this shortcoming by quantifying isolated muscle activation through recordings of summated motor unit action potentials from electrodes placed on the skin over superficial muscles.¹⁴ Zaneb et al.¹⁵ used sEMG to quantify back muscle activity during treadmill trot and detected significantly lower amplitude ratios bilaterally from longissimus dorsi (longissimus) in a group of horses with chronic, unilateral HL lameness. They interpreted this finding as a 'more distinct resting phase' between active contractions of longissimus.¹⁵ Unfortunately, axial movement was not quantified to corroborate this interpretation and comparisons were drawn from horses with subjectively assessed and nonstandardised lameness. In recognition of this, we have therefore initiated research to directly compare appendicular¹⁶ and axial movement and muscle activity between nonlame and standardised lameness conditions during overground locomotion.

This study aimed to quantify and compare thoracolumbar and pelvic kinematics and longissimus activity in horses' thoracic and lumbar regions during overground trot in nonlame and induced forelimb (iFL) and hindlimb (iHL) lameness conditions. Based on previously reported

findings and clinical observations, we hypothesised that there will be different adaptations during iFL and iHL, with the changes in ROM and longissimus activity being more localised to the thoracic and lumbar regions, respectively.

2 | MATERIALS AND METHODS

2.1 | Horses

Eight horses (mean \pm SD age: 9.2 \pm 3.9 years, height: 161.3 \pm 3.4 cm, body mass: 582.1 \pm 39.4 kg, 7 mares, 1 stallion) were used. Horses were in regular ridden exercise, were accustomed to being walked and trotted in-hand, and were deemed clinically nonlame (<1/5 AAEP Lameness Scale) through visual assessments by two equine veterinarians (TS, FSB).

2.2 | Kinematic instrumentation

Three-dimensional (3D) kinematic data were collected using an optical motion capture (OMC) system of 18 high-speed infrared cameras (Oqus 700+, Qualisys AB). The OMC system was hardware synchronised to the sEMG system and recorded time series for both data types in one file for further processing. The calibrated volume for data collection was 56 m long and 10 m wide. Super-spherical, retro-reflective markers (Qualisys AB, 19 mm diameter) were attached over anatomical landmarks, as presented in Figure S1A. Individual markers and a marker cluster on the head were attached using double-sided adhesive tape, with an additional drop of cyanoacrylate glue used for the hoof and limb markers.

2.3 | Surface electromyography instrumentation

The sEMG data were collected bilaterally from longissimus using wireless sEMG sensors (Trigno, Delsys Inc.) with a fixed interelectrode distance of 10 mm. Ultrasonography was used for the detection of the desired locations over longissimus, at the T14 and L1 vertebrae, 6 cm lateral to midline.¹⁷ Once identified, each skin location was clipped of hair, then thoroughly cleaned using isopropyl alcohol. A small amount of electrolytic solution (0.9% saline) was applied to each electrode before attaching sensors to the prepared skin locations using double-sided adhesive interface strips (Delsys Inc.), with the electrodes oriented perpendicular to the

underlying muscle fibre direction.^{18,19} Additional adhesion included a drop of cyanoacrylate glue on the double-sided tape, attached to the top and bottom of the sensor, above each electrode pair (Figure S1B).

2.4 | Data collection

To simulate a real-world lameness examination, sEMG (2000 Hz) and 3D kinematic (200 Hz) data were synchronously collected from in-hand trot trials, conducted on a straight, hard, indoor runway during control and induced lameness (iFL, iHL) conditions. Four trials (passes down the runway) were conducted per condition. Data were initially collected from the control condition to determine the baseline gait pattern of each horse (baseline 1). Then, mild iFL (2–3/5 AAEP Lameness Scale) was temporarily induced by mechanical screw pressure applied to the sole of the hoof using a modified horseshoe.²⁰ Lameness induction was applied, graded, and monitored by veterinarians (TS, FSB). Horses were randomly divided into two groups ($n = 4$) for right and ($n = 4$) left iFL, in a cross-over design. Following iFL, trot trials were repeated. After a washout period of at least 24 h, the same data collection process was repeated for baseline 2 and iHL conditions, where iHL was again randomised to the right ($n = 4$) or left ($n = 4$) HL.

2.5 | Data processing and analysis

2.5.1 | Kinematic processing and analysis

Stride segmentation was based on the detection of gait events using kinematic data as described by Roepstorff et al.²¹ Upper body vertical displacement of poll, withers and pelvis were high-pass filtered (Butterworth fourth order) with the cut-off frequency adjusted to the stride frequency of each measurement.²² Kinematic variables were calculated as previously described for upper body asymmetry²³ and for thoracolumbar and pelvic motion⁶ and are described in detail in Figure S2. Briefly, the thoracolumbar angle was calculated using cranial and caudal segments, defined using markers located on the T6 and T13 vertebrae, and on the T13 vertebra and the tuber sacrale, respectively. Thoracolumbar flexion/extension angle was defined in the sagittal plane with flexion as positive and extension as negative, and lateral bending angle was defined in the transverse plane, with bending to the LS (lame side) as positive and NLS (nonlame side) as negative.⁶ For the pelvic segment, pitch and yaw were defined relative to a line between the withers and tuber sacrale markers, with roll defined relative to the horizontal.⁶ Pelvis pitching rotations were defined as negative during flexion and positive for extension and pelvis roll and yaw rotations were defined as downward (ventral) and forward (cranial) movements of the tuber coxae on the LS and NLS, respectively.⁶

In order to progress to further data analysis, the measured motion asymmetry differences between an individual horse's baseline and

lameness induction had to exceed previously described reference values for upper body motion asymmetry of 13 mm for head movement (MinDiff Poll or MaxDiff Poll) and 5 mm for hindquarter (pelvic) motion (MinDiff Pelvis and/or MaxDiff Pelvis) and with standard deviations less than their respective means.²⁴

2.5.2 | Surface electromyography data processing and analysis

Raw sEMG signals were DC-offset removed, high-pass filtered (Butterworth fourth order, 40 Hz cut-off),²⁵ and full-wave rectified. Discrete sEMG variables were calculated for each stride and included the average rectified value (ARV) and timings of sEMG activity onset, offset, and resultant activity duration for each muscle location.

ARV was calculated from full-wave rectified signals using stride duration as the temporal domain. As NLS and LS of longissimus were analysed separately, contralateral HL impact events were employed for stride segmentation for sEMG variables. Outliers in ARV data, defined as 2 standard deviations outside the mean ARV values within each horse, muscle location, and condition, were excluded from further analysis. To ensure that the same strides were analysed within the LS and NLS for each condition and muscle location, detected outlier strides were excluded for both muscle locations (T14 and L1) within that stride. To reduce intersubject variability, within-horse ARV data were normalised to a reference voluntary contraction (RVC) defined as the maximum value observed for each muscle location relative to the corresponding baseline condition.²⁶ This permitted examination of the proportional change in muscle activity between baselines and the corresponding iFL/iHL conditions.

Muscle activity onset and offset events were calculated across strides, in accordance with the double threshold method.²⁷ Events were calculated from enveloped signals (Butterworth fourth order, low-pass filter, 10 Hz cut-off), with an amplitude threshold defined as 20% of the peak amplitude value of each individual sEMG signal and the timing threshold defined as 5% of the average gait cycle duration from the control condition across all horses.²⁷ Given the variation in baseline activity amplitude for longissimus signals and in accordance with St. George et al.,²⁷ the amplitude threshold was increased or reduced by 5% to improve accuracy for certain horse/muscle combinations. Onset, offset, and resultant activity duration for each muscle were normalised to percentage stride duration.

To complement the discrete variables, continuous sEMG data, in the form of time and amplitude-normalised sEMG signals across all strides/conditions were prepared for analysis.²⁸ Within-horse, enveloped sEMG signals (Butterworth fourth order, low-pass filter, 25 Hz cut-off) were normalised to an RVC: the peak amplitude value of enveloped signals, observed for each muscle location across all strides (excluding detected outlier strides) from the corresponding baseline condition. As the RVC represents a submaximal contraction, it was possible for both normalised ARV and continuous data from the iFL/iHL conditions to exceed 100% of the RVC.

2.6 | Data analysis

To increase statistical power, asymmetry parameters from right iFL and iHL were multiplied by -1 to mirror the indices and thus categorise all data as if they were derived from left limb inductions only. For the remaining variables, including sEMG variables, data from right iFL and iHL, were also mirrored. Therefore, all results are reported as results of the lame side (LS) and the nonlame side (NLS). The original kinematic values, without the mirroring procedure applied, are presented in Table S1.

Linear mixed models were used to estimate the effect of lameness induction. iFL and iHL were modelled separately. Stride level data for discrete kinematic and sEMG variables were entered into the model for the baseline condition and the corresponding induced lameness conditions (baseline 1 and iFL, baseline 2 and iHL) from each horse. Models were calculated in open-source R-studio (version 3.6.3) using the package lme4 (version 1.1-15), with horse ID as a random effect and condition as fixed effect. Additionally, separate models were conducted to evaluate the impact of speed on results, using speed as a random slope to correct for this variable. Model fit was assessed using q - q plots and boxplots of the residuals. For each model, results are presented as estimated marginal means, standard error (SE) and 95% lower and upper confidence intervals calculated using the software package emmeans (version 1.7.1). Significance values were corrected for multiple comparisons using the false discovery rate method.

Statistical parametric mapping (SPM), a technique increasingly used to investigate differences in ambulatory behaviour, was employed to analyse continuous kinematic and sEMG data, (ie, complete time series of the normalised signals from one stride).²⁸⁻³⁰ Time and amplitude normalised stride values for sEMG data and angle-time curves for kinematic data were assembled into $1 \times 101 \times 1$ vector fields (median stride, 101 datapoints per stride and one dimension per data point) for each signal, condition, and horse. The open source spm1d package (version M.0.4.1) was used to conduct SPM analysis in Matlab (version 2020b).²⁹ For both sEMG and kinematic data, separate analyses were performed to compare signals between baseline and the corresponding iFL/iHL conditions. For group-level kinematic and sEMG data, paired samples t -tests were performed. For individual sEMG data, Hotelling's T2 tests were performed on T14 and L1 locations together, but separately for the LS and NLS. If significant results were found in a Hotelling's T2 test, paired samples t -tests were performed as post hoc analyses. The two-tailed significance level was set at $\alpha = 0.05$ and p values were adjusted for multiple comparisons using the Bonferroni correction.

3 | RESULTS

3.1 | General descriptive findings

Thoracolumbar movement and longissimus activation patterns during trot are presented in a (Video S1), containing the moving 3D model

and associated kinematic and sEMG signals from a representative horse during the baseline 1 condition. A total of 647 strides were used for kinematic analysis (163: baseline 1, 132: baseline 2, 189: iFL and 163: iHL). A total of 508 and 504 strides were employed for the separate sEMG analysis of the LS (138: baseline 1 and iFL, 116: baseline 2 and iHL) and NLS (136: baseline 1 and iFL, 116: baseline 2 and iHL), respectively. Across all horses, muscle locations and conditions, a biphasic activation pattern was observed for longissimus, with activation bursts consistently occurring between $33.1 \pm 4.8\%$ to $51.8 \pm 4.7\%$ and $84.3 \pm 4.5\%$ to $100.9 \pm 4.6\%$ of stride duration. Additional bursts or elongation of the bi-phasic pattern were observed, albeit less consistently, at $13.5 \pm 4.0\%$ to $24.6 \pm 4.8\%$ and $64.6 \pm 3.9\%$ to $75.5 \pm 3.7\%$ of stride duration. Linear mixed model results for iFL and iHL are presented in Tables 1 and 2, with sEMG activation timings presented separately in Table S2. To allow for comparison of the effect of speed on results, the following sections include data from both models, with (Tables 1 and S2) and without (Tables 2 and S2) statistical correction for speed. Unless otherwise stated, this section describes results from the speed-corrected model. Statistical correction for speed has not been applied to the continuous time-series data presented in Figures 1-6.

3.2 | Effect of forelimb lameness induction

3.2.1 | Kinematic parameters

An increase in most asymmetry variables was found for iFL (Tables 1 and 2, S1), mainly Poll MinDiff (53.73 mm, $p < 0.001$) and Withers MinDiff (13.14 mm, $p < 0.001$). Changes in thoracolumbar motion for iFL were characterised by a significant decrease in peak flexion angle ($p < 0.05$), and slight, but nonsignificant decreases in peak extension and peak left and right lateral bending angles (Table 1, Figures 1 and 2). Changes in pelvic motion were characterised by a significant increase in pitch ($p < 0.0001$) and nonsignificant decreases in pelvis yaw and roll (Table 1, Figure 3). Nonspeed corrected findings (Table 2) were similar except for pelvis yaw ROM, which increased significantly ($p < 0.05$) without speed-correction. SPM results for kinematic data from the thoracolumbar and pelvic segments for the group of horses are presented in Figures 2A,B and 3A-C, respectively, and showed no significant differences between conditions.

3.2.2 | Surface electromyography parameters

Significant increases ($p < 0.0001$) and decreases ($p < 0.05$) in ARV were respectively observed at the LS and NLS L1 sites during iFL, but changes in ARV at T14 locations were nonsignificant when compared with baseline (Table 1). Activity duration of longissimus significantly increased ($p < 0.0001$) at the LS, T14 site, but was not significantly altered at the other locations. In general, onset/offset timings were not significantly influenced by iFL (Figure 1, Table S2) and any significant alterations in timings were not restricted to specific activation

TABLE 1 Speed corrected data as estimated marginal means (EM mean) and standard error (SE) for discrete variables from baseline and iFL and iHL lameness conditions and estimated mean marginal differences (EM mean difference, EM mean % difference) between corresponding baseline and induced lameness conditions and associated *p* values

Variable	Induction	Baseline		Induction		EM mean difference	EM mean % difference	<i>p</i> value
		EM mean	SE	EM mean	SE			
Stride duration (s)	FL	0.77	0.01	0.75	0.01	-0.01	1.30	<0.001
	HL	0.73	0.01	0.71	0.01	-0.02	2.74	<0.001
Asymmetry variables (mm)								
MinDiff Poll	FL	-3.36	5.30	-57.09	5.22	-53.73	n/a	<0.001
	HL	-5.72	5.17	-13.85	5.10	-8.13	n/a	<0.001
MaxDiff Poll	FL	-7.18	5.38	-29.47	5.72	-22.29	n/a	<0.001
	HL	-2.87	3.04	-11.95	2.92	-9.08	n/a	<0.001
MinDiff Withers	FL	-2.36	1.64	-15.51	1.75	-13.14	n/a	<0.001
	HL	-2.07	1.70	10.96	1.72	13.04	n/a	<0.001
Mindiff Pelvis	FL	1.03	1.14	3.25	1.29	2.22	n/a	<0.001
	HL	0.34	2.68	-21.91	2.67	-22.25	n/a	<0.001
Maxdiff Pelvis	FL	0.68	3.27	6.29	3.28	5.61	n/a	<0.001
	HL	4.78	1.37	-23.08	1.39	-27.87	n/a	<0.001
Hip hike Swing	FL	0.81	4.22	13.98	4.23	13.17	n/a	<0.001
	HL	2.89	6.31	-58.84	6.33	-61.73	n/a	<0.001
Maximum thoracolumbar angle (degrees)								
Left/LS lateral bending	FL	4.41	0.71	4.39	0.73	-0.02	0.45	0.9
	HL	3.54	1.00	2.91	1.00	-0.63	17.80	<0.001
Right/NLS lateral bending	FL	-2.14	0.74	-2.04	0.77	0.11	5.14	0.7
	HL	-3.37	1.00	-4.26	1.00	-0.89	26.41	<0.001
Extension	FL	-23.75	1.13	-23.67	1.08	0.07	0.29	0.6
	HL	-21.03	1.10	-21.64	1.11	-0.61	2.90	<0.001
Flexion	FL	-16.36	0.85	-16.56	0.85	-0.20	1.22	0.03
	HL	-15.97	0.91	-16.34	0.91	-0.36	2.25	<0.001
Pelvic ROM (degrees)								
Pitch	FL	7.88	0.57	8.39	0.57	0.50	6.35	<0.001
	HL	8.49	0.66	9.27	0.66	0.77	9.07	<0.001
Roll	FL	7.53	0.78	7.40	0.77	-0.13	1.73	0.4
	HL	7.26	0.68	7.10	0.67	-0.16	2.20	0.4
Yaw	FL	3.20	0.33	3.10	0.33	-0.10	3.12	0.07
	HL	3.32	0.21	3.45	0.21	0.12	3.61	<0.001
Longissimus sEMG ARV (%)								
T14, NLS	FL	97.33	4.53	93.89	4.92	-3.44	3.5	0.09
	HL	82.29	6.83	108.23	6.78	25.94	31.52	<0.001
T14, LS	FL	91.19	1.78	88.78	1.96	-2.41	2.6	0.1
	HL	79.95	5.43	117.52	5.25	37.58	47	<0.001
L1, NLS	FL	93.05	1.53	89.35	1.76	-3.70	4.0	0.03
	HL	89.99	5.53	111.17	5.59	21.18	23.54	<0.001
L1, LS	FL	116.57	22.05	193.35	24.75	76.78	65.9	<0.001
	HL	84.73	4.35	97.23	4.31	12.50	14.75	<0.001

Bold text indicates significant differences between baseline and induced lameness conditions ($p < 0.05$).

bursts, occurring both earlier and later across sensor sites (Table S2). Contrasting sEMG results were observed between models with- and without statistical correction for speed (Table 2 and S2). For example,

significant increases in ARV from the T14 site on the NLS and LS were observed during iFL ($p > 0.0001$) when speed was not corrected for (Table S2). Significant differences in activity onset/offset timings were

TABLE 2 Nonspeed corrected data as estimated marginal means (EM mean) and standard error (SE) for discrete variables from baseline and iFL and iHL lameness conditions and estimated mean marginal differences (EM mean difference, EM mean % difference) between corresponding baseline and induced lameness conditions and associated *p* values

Variable	Induction	Baseline		Induction		EM mean difference	EM mean % difference	<i>p</i> value
		EM mean	SE	EM mean	SE			
Stride speed (m/s)	FL	3.13	0.10	2.87	0.10	-0.26	8.31	<0.001
	HL	3.09	0.12	3.03	0.12	-0.06	1.94	0.02
Stride duration (s)	FL	0.74	0.02	0.78	0.02	0.04	5.41	<0.001
	HL	0.75	0.01	0.74	0.01	-0.01	1.33	<0.001
Asymmetry variables (mm)								
MinDiff Poll	FL	-3.99	4.42	-57.35	4.41	-53.36	n/a	<0.001
	HL	-3.04	3.19	-14.28	3.09	-11.25	n/a	<0.001
MaxDiff Poll	FL	-4.62	6.26	-24.27	6.25	-19.65	n/a	<0.001
	HL	-3.40	2.14	-13.07	2.04	-9.68	n/a	<0.001
MinDiff Withers	FL	-1.97	2.06	-14.13	2.06	-12.16	n/a	<0.001
	HL	-2.61	1.75	11.23	1.73	13.84	n/a	<0.001
MinDiff Pelvis	FL	-0.65	1.75	0.79	1.75	1.44	n/a	0.05
	HL	1.40	2.13	-21.24	2.11	-22.64	n/a	<0.001
MaxDiff Pelvis	FL	3.46	1.34	9.31	1.32	5.85	n/a	<0.001
	HL	5.60	2.55	-25.74	2.52	-31.34	n/a	<0.001
Hip Hike Swing	FL	3.92	2.33	16.72	2.32	12.80	n/a	<0.001
	HL	7.51	5.03	-56.32	4.98	-63.83	n/a	<0.001
Maximum thoracolumbar angle (degrees)								
Left/LS lateral bending	FL	4.53	0.65	4.72	0.65	0.19	4.19	0.4
	HL	4.20	0.80	3.26	0.80	-0.94	22.38	<0.001
Right/NLS lateral bending	FL	-2.10	0.70	-2.27	0.70	-0.17	8.10	0.4
	HL	-2.84	0.93	-3.93	0.93	-1.09	38.38	<0.001
Extension	FL	-22.54	0.96	-22.72	0.96	-0.18	0.80	0.2
	HL	-21.82	1.05	-22.50	1.05	-0.68	3.12	<0.001
Flexion	FL	-16.62	0.83	-16.91	0.83	-0.29	1.74	<0.001
	HL	-16.00	0.80	-16.33	0.80	-0.32	2.00	<0.001
Pelvis ROM (degrees)								
Pitch	FL	8.39	0.48	9.13	0.48	0.73	8.70	<0.001
	HL	8.63	0.42	9.68	0.42	1.05	12.17	<0.001
Roll	FL	7.12	0.66	7.25	0.66	0.12	1.69	0.4
	HL	7.25	0.63	7.21	0.63	-0.04	0.55	0.8
Yaw	FL	3.02	0.32	3.30	0.32	0.28	9.27	0.02
	HL	3.16	0.23	3.23	0.23	0.07	2.22	0.2
Longissimus sEMG ARV (%)								
T14, NLS	FL	86.73	6.09	80.30	6.09	-6.43	7.41	<0.001
	HL	85.08	4.83	109.81	4.81	24.73	29.07	<0.001
T14, LS	FL	88.01	3.31	82.65	3.31	-5.36	6.09	<0.001
	HL	86.66	5.73	118.28	5.72	31.62	36.49	<0.001
L1, NLS	FL	86.76	3.75	78.91	3.75	-7.85	9.05	<0.001
	HL	83.12	4.00	101.76	3.98	18.64	22.43	<0.001
L1, LS	FL	92.48	30.70	166.55	30.68	74.07	80.09	<0.001
	HL	86.28	2.77	95.08	2.77	8.81	10.21	<0.001

Bold text indicates significant differences between baseline and induced lameness conditions (*p* < 0.05).

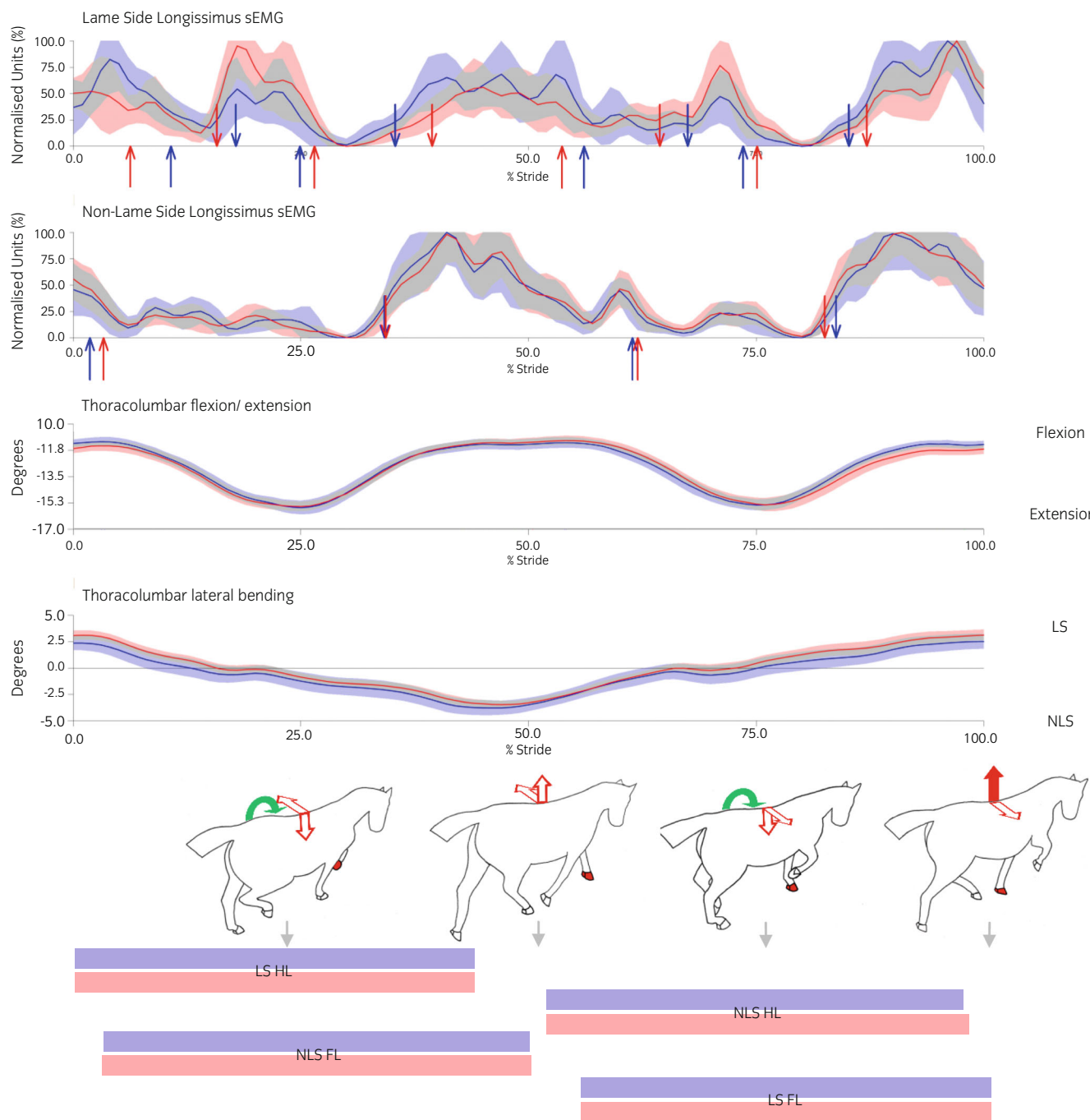


FIGURE 1 Graphs show mean (solid line) and standard deviation (shaded area) of amplitude-normalised, linear-enveloped sEMG signals from LS and NLS longissimus (L1 location) and time-angle curves for thoracolumbar flexion/extension and lateral bending from representative ‘Horse 4’ during baseline 1 (blue) and iFL (red) conditions. Within the sEMG graphs, upward and downward arrows demarcate sEMG activity onset and offset, respectively, for baseline 1 (blue arrows) and iFL (red arrows). Data are time-normalised between LS hindlimb impact events. Line drawings show the outline of the horse at different stages of the stride cycle, as illustrated by horizontal bars showing mean stance phase for each limb (baseline 1: blue bars, iFL: red bars). Within the line drawings, red arrows illustrate significant (solid arrows) and nonsignificant (outline arrows) decreases in thoracolumbar flexion/extension (vertical arrows) and lateral bending (horizontal arrows) following iFL. Significant increases in pelvic pitching are illustrated as curved, green arrows around the transverse axis

also observed more frequently in the nonspeed corrected model (Table S2).

The sEMG waveforms from individual horses showed significant differences between conditions when analysed using SPM, as

illustrated by ‘Horse 4’ in Figure S3. SPM post hoc analysis of LS sEMG data revealed that significant differences between conditions are primarily influenced by significant increases in amplitude at the L1 location (Figure S3). However, when sEMG data were grouped across

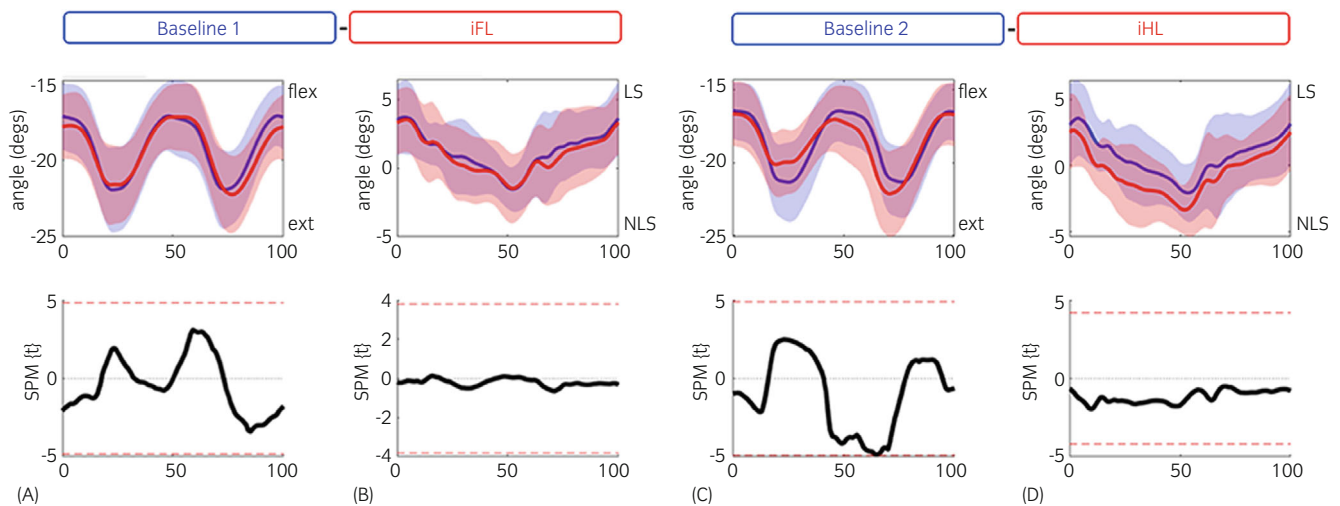


FIGURE 2 Statistical parametric mapping (SPM) results for time-normalised thoracolumbar kinematic data across the group of horses for flexion/extension (A,C) and lateral bending (B,D) during baseline 1 and iFL (A,B) and baseline 2 and iHL (C,D). Upper graphs illustrate median (solid line) and standard deviation (shaded area) kinematic data for baseline (blue) and induced lameness (red) conditions. Lower graphs illustrate the paired samples t-test SPM result (black solid line) and the critical thresholds for significance (red dashed line). Data are time-normalised between impacts of the LS hindlimb

all horses, SPM results revealed that such differences were not significant (Figure 4).

3.3 | Effect of hindlimb lameness induction

3.3.1 | Kinematic parameters

An increase in most asymmetry variables was found for iHL (Tables 1 and 2, Table S1), mainly pelvis MinDiff (22.25 mm, $p < 0.001$), pelvis MaxDiff (27.87 mm, $p < 0.001$) and Hip Hike Swing (61.73 mm, $p < 0.001$). Changes in thoracolumbar motion were characterised by a significantly larger peak extension angle and significantly smaller peak flexion angle ($p < 0.0001$) (Figure 5, Table 1). Peak lateral bending angle significantly decreased ($p < 0.001$) and increased ($p < 0.0001$) on the LS and NLS, respectively (Figure 5, Table 1). Changes in pelvic motion were characterised by a significant increase in pitch and yaw ($p < 0.0001$), and nonsignificant changes in roll ($p > 0.05$) (Figure 3D–F, Table 1). Results from the nonspeed corrected model (Table 2), were congruent with results from the speed corrected model (Table 1) except for pelvis yaw ROM, which was nonsignificant when speed was not corrected for. SPM results showed no significant differences between conditions for thoracolumbar motion (Figure 2C,D), but significant differences were observed for pelvis pitch and roll during the lame diagonal stance (Figure 3D,E) ($p < 0.05$).

3.3.2 | Surface electromyography parameters

Significant increases in ARV were observed bilaterally at T14 and L1 longissimus sites ($p < 0.0001$) (Table 1). At both T14 and L1, activation

onset/offset events were generally detected significantly earlier in the stride cycle on the LS, and later on the NLS ($p < 0.05$) (Figures 5 and 6, Table S2). On the LS, longissimus activity duration significantly increased at T14 ($p < 0.0001$) and decreased at L1 ($p < 0.0001$) (Table S2). ARV and sEMG activation timing results from the non-speed corrected model (Table 2, Table S2), were congruent with results from the speed corrected model (Table 1 and S2), except for two activation events, which showed significant differences between conditions ($p < 0.05$) when speed was not corrected for (Table S2).

The sEMG waveforms from individual horses showed significant differences between conditions when analysed using SPM, as illustrated in ‘Horse 6’ (Figure S4), but when sEMG data were grouped across all horses, SPM results revealed that such differences were not significant (Figure 6).

4 | DISCUSSION

This study combined motion capture and sEMG technology to quantify and compare thoracolumbar and pelvic kinematics and longissimus activity, between baseline and standardised iFL and iHL conditions. Kinematic asymmetry indices provided quantitative evidence for the successful induction of iFL and iHL across all horses, which resulted in different, significant changes in thoracolumbar and pelvic ROM, and longissimus muscle activity. iFL was characterised by significant decreases in peak thoracolumbar flexion and increases in pelvis pitching ROM (Figure 1). These adaptations were also observed during iHL, plus significant increases on LS and decreases on NLS in peak thoracolumbar lateral bending angle and increases in peak thoracolumbar extension angle and pelvis yaw ROM (Figure 5). Clear adaptations in longissimus activation patterns were observed during iHL, with

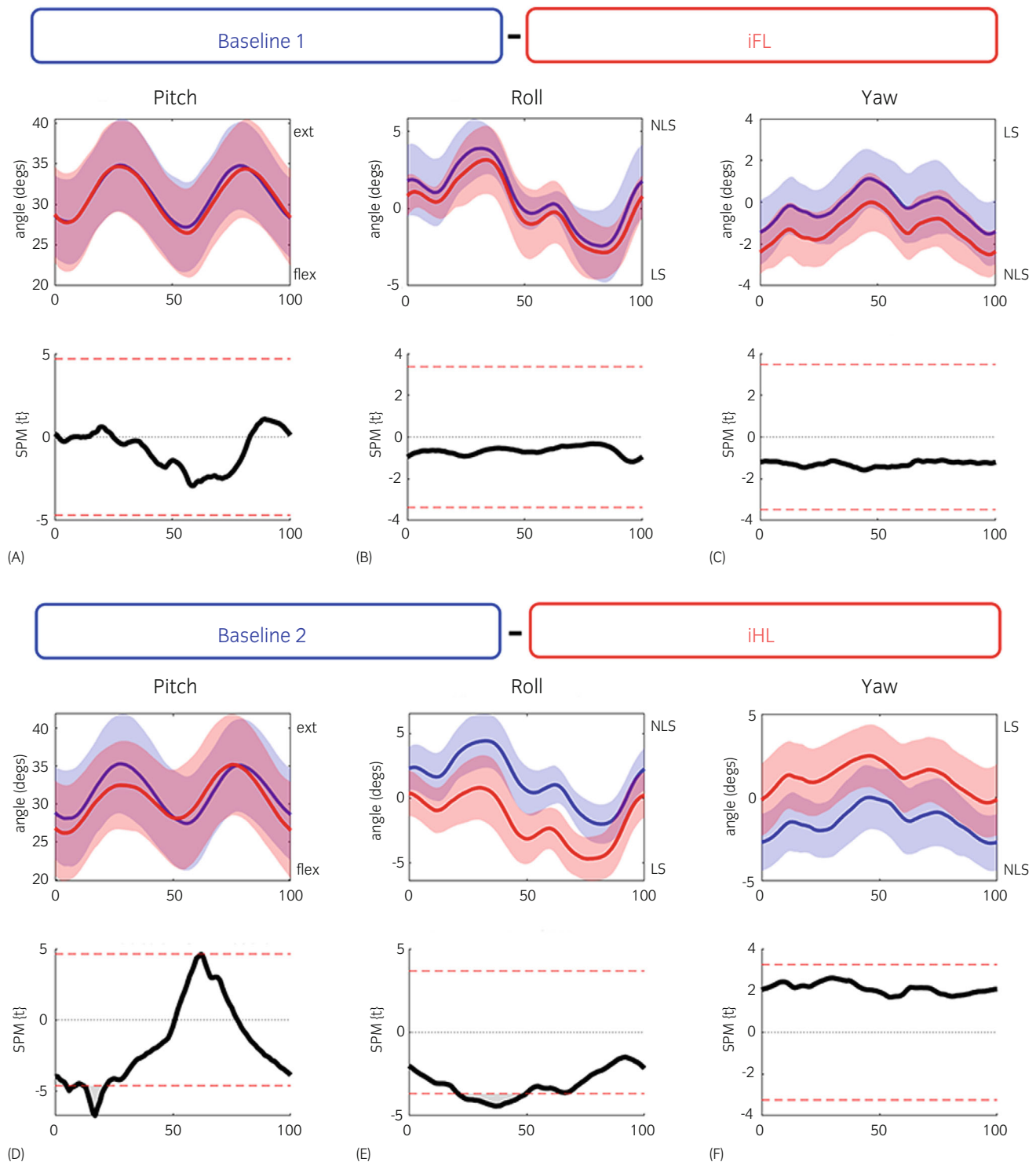


FIGURE 3 Statistical parametric mapping (SPM) results for time-normalised pelvis segment kinematics across the group of horses for pitch (A,D), roll (B,E), yaw (C,F) during baseline 1 and iFL (A-C), and baseline 2 and iHL (D-F). Within each subpanel, upper graphs illustrate median (solid line) and standard deviation (shaded area) kinematic data for baseline (blue) and induced lameness (red) conditions. Lower graphs illustrate the paired samples t-test SPM result (black solid line) and the critical thresholds for significance (red dashed line). Data are time-normalised between impacts of the LS hindlimb. Grey shaded areas indicate regions with statistically significant differences between conditions

significant bilateral increases in amplitude across T14 and L1 and distinct phasic shifts reflecting precipitated (LS) and delayed (NLS) muscle activation onset/offset within the stride cycle. In comparison,

adaptations in longissimus activation patterns did not generally change during iFL, with no distinct phasic shifts in activation observed, but with significant changes in amplitude only observed at

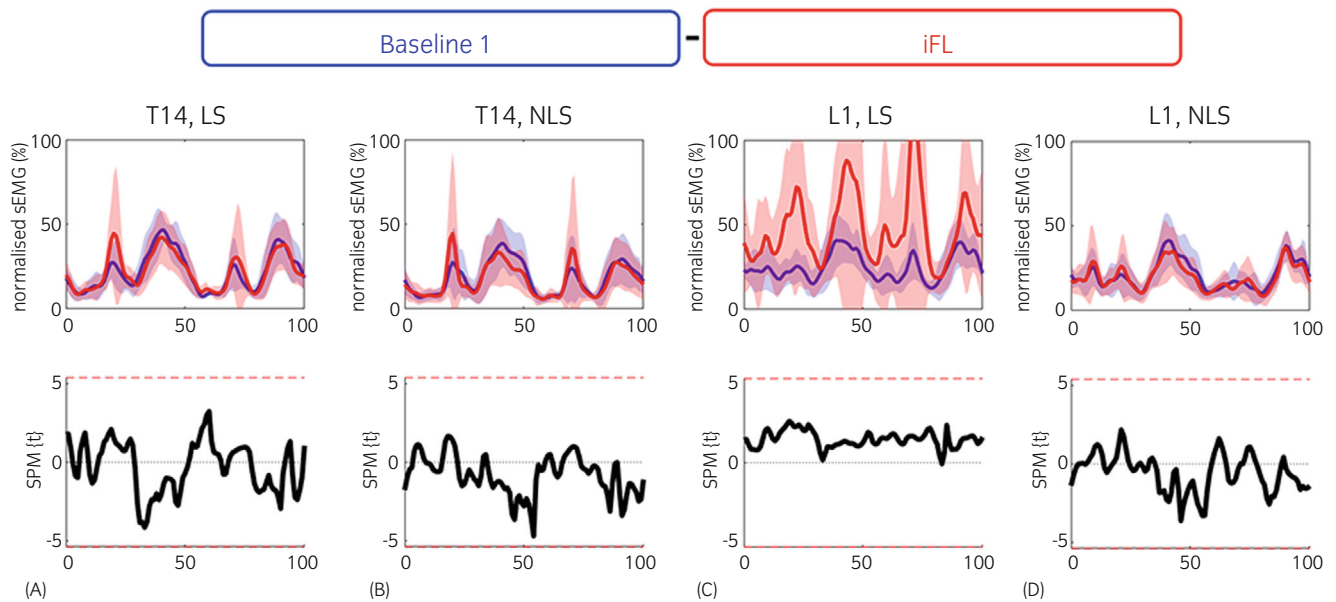


FIGURE 4 Statistical parametric mapping (SPM) results for time and amplitude-normalised longissimus sEMG data across the group of horses during baseline 1 (blue) and iFL (red) conditions for T14 (A,B) and L1 (C,D) locations on the LS (A,C) and NLS (B,D). Within each subpanel, upper graphs illustrate median (solid line) and standard deviation (shaded area) sEMG data and lower graphs illustrate the paired samples *t*-test SPM result (black solid lines) and the critical thresholds for significance (red dashed line). Data are time normalised between ipsilateral hindlimb impact events

the L1 locations. Therefore, findings from this study support the hypothesis that iFL and iHL cause different adaptations in thoracolumbar and pelvic ROM and longissimus activity, but do not support the hypothesis that these changes are localised to the thoracic and lumbar areas during iFL and iHL, respectively.

4.1 | Kinematic adaptations of thoracolumbar and pelvic motion during iFL and iHL

The overall finding that mild, reversible iFL and iHL result in different measurable adaptations in thoracolumbar and pelvic motion agrees with previous studies that reported increases in overall thoracolumbar flexion/extension ROM during iFL,¹⁰ but no significant differences during iHL.¹¹ In contrast, horses in this study adapted to iFL by significantly decreasing peak thoracolumbar flexion during LS stance phase (Figures 1 and 2A), without significantly altering peak extension or lateral bending angles, and to iHL by significantly decreasing peak thoracolumbar flexion and increasing extension (Figures 2C and 5). Comparisons between studies are limited by methodological differences in data processing and analysis and the fact that horses were evaluated during treadmill locomotion, in which thoracolumbar motion differs from overground locomotion.^{10,11,31,32} However, our findings are congruent with clinical observations of increased stiffness/decreased flexibility of the thoracolumbar region in horses presenting FL and HL lameness. Further, our findings for iHL (Figure 2C) agree with a descriptive study that reported decreased extension during LS stance and increased extension during NLS stance in a single clinical hindlimb lameness case

(right tarsal osteoarthritis) compared with a nonlame horse during overground trot.³³

Gómez-Álvarez et al.¹⁰ related compensatory ‘head nod’ during iFL and its concurrent effects on thoracic flexion/extension to significant increases in extension angles of individual thoracic and lumbar vertebrae during lame diagonal stance. Indeed, an examination of group-averaged iFL time-angle curves in Figure 2A reveals a general, albeit nonsignificant, trend for increased extension and decreased flexion during lame diagonal stance. Thus, asymmetrical head and neck movement during iFL appears to affect the subtle, but largely nonsignificant, asymmetries observed in group-averaged thoracolumbar flexion/extension. Discrete data revealed that peak thoracolumbar flexion was significantly decreased during iFL and based on Figure 2A, this was attributed to the flexion peak bridging at the end of lame and nonlame diagonal stance phases (Figure 1). Significant increases in thoracic flexion, as observed by Gómez-Álvarez et al.¹⁰ during nonlame diagonal stance, were not found in this study for group-averaged data, although individual kinematic data reveals that certain horses exhibited this movement pattern, particularly the two horses with the highest MinDiff Poll values (i.e., the highest degree of iFL) (Table S1). Significant increases in T10 and T13 lateral bending angles towards the LS during lame diagonal stance have been observed and interpreted as an attempt to shift the centre of mass towards the NLS.¹⁰ Again, group-averaged lateral bending data from our study does not support this finding, but individual horses exhibited increased lateral bending towards the LS. Thus, in accordance with known interhorse variance in back motion during nonlame locomotion,^{6,8,34} findings from this study suggest that individual horses adopt different adaptation strategies, most notably during iFL.

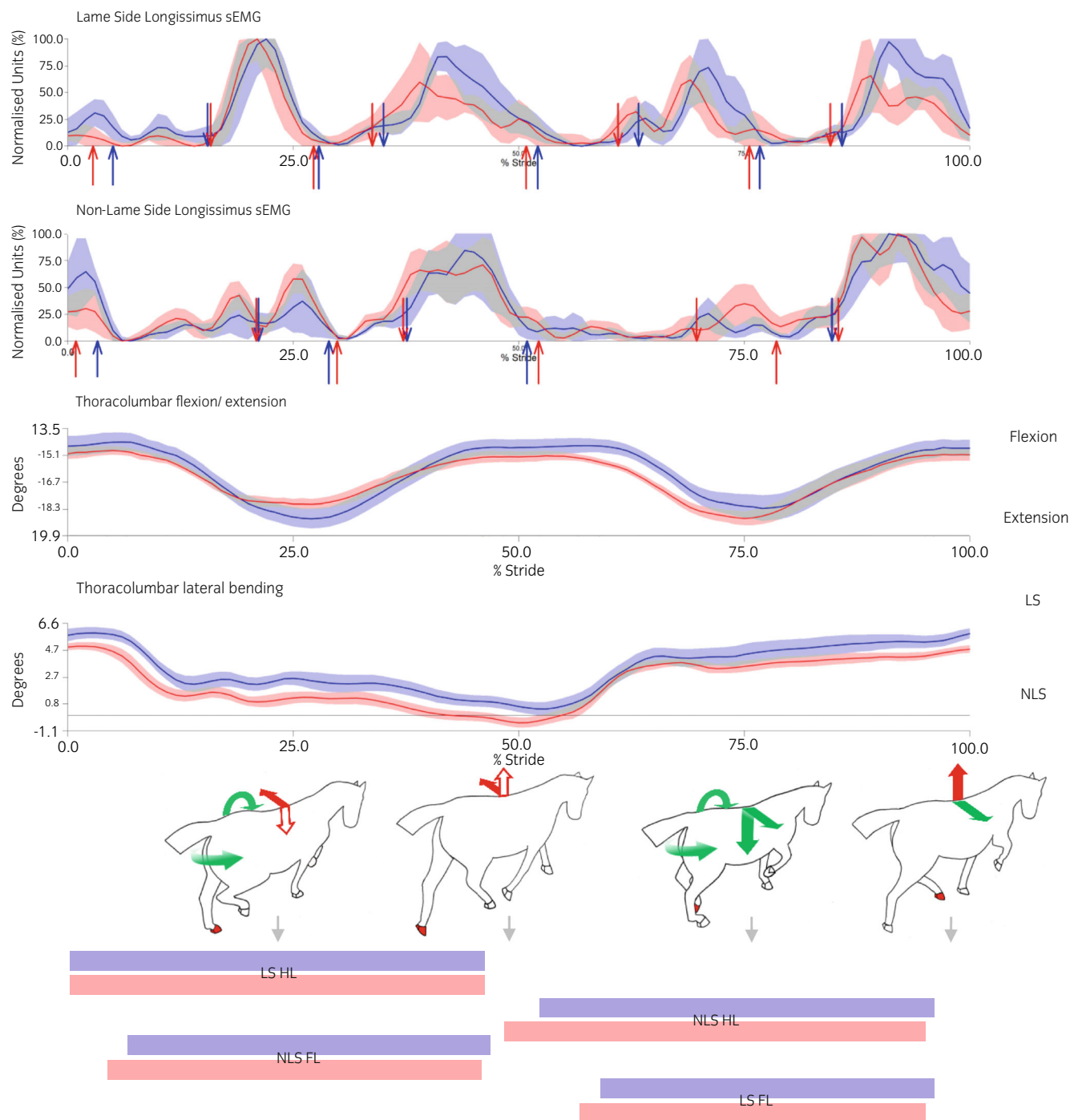


FIGURE 5 Graphs show mean (solid line) and standard deviation (shaded area) of amplitude-normalised, linear enveloped sEMG signals from LS and NLS longissimus (L1 location) and time-angle curves for thoracolumbar flexion/extension and lateral bending from representative 'Horse 2' during baseline 2 (blue) and iHL (red) conditions. Within the sEMG graphs, upward and downward arrows demarcate sEMG activity onset and offset, respectively, for baseline 2 (blue arrows) and iHL (red arrows). Data are time-normalised between LS hindlimb impact events. Line drawings show the outline of the horse at different stages of the stride cycle, as illustrated by horizontal bars showing mean stance phase for each limb (baseline 2: blue bars, iHL: red bars). Within the line drawings, arrows illustrate significant (solid arrows) and nonsignificant (outline arrows) increases (green arrow) and decreases (red arrow) in thoracolumbar flexion/extension (vertical arrows) and lateral bending (horizontal arrows) following iHL. Significant increases in pelvis pitch and yaw are illustrated as curved, green arrows around the transverse and vertical axes, respectively

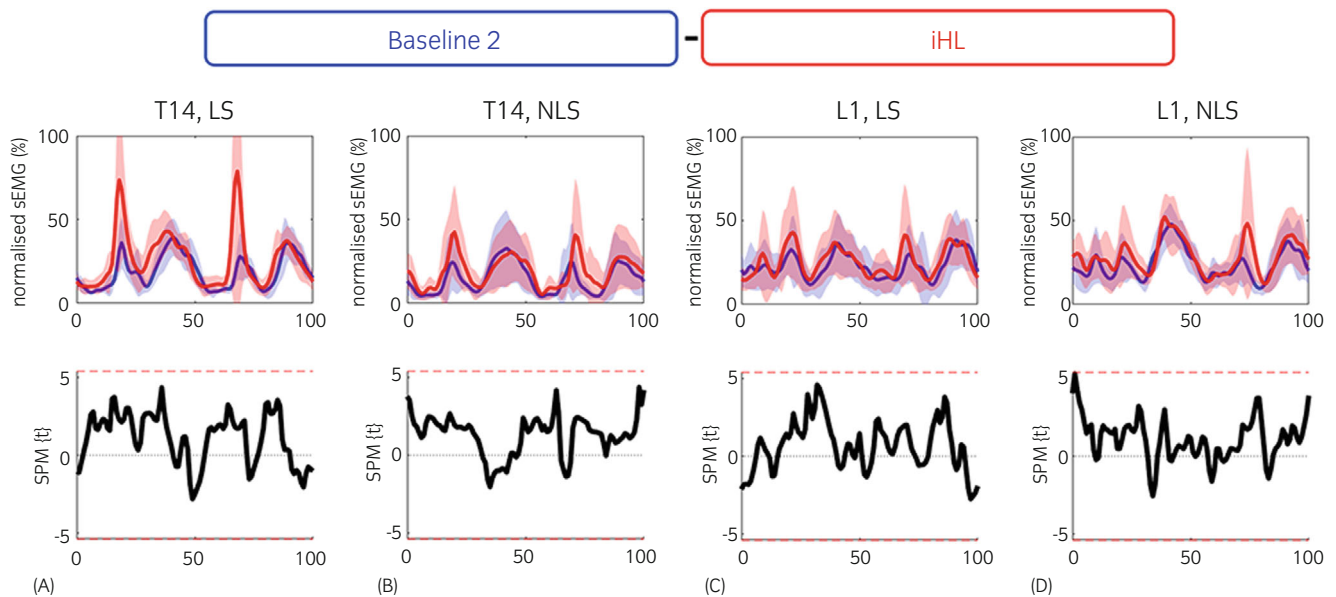


FIGURE 6 Results of SPM of time and amplitude normalised sEMG data from longissimus across the group of horses during baseline 2 (blue solid line/shaded area) and iHL (red solid line/shaded area) for T14 (A,B) and L1 (C,D) locations on the LS (A,C) and NLS (B,D). Within each subpanel, upper graphs illustrate median (solid line) and standard deviation (shaded area) sEMG data and lower graphs illustrate the paired samples *t*-test SPM result (black solid lines) and the critical thresholds for significance (red dashed line). Data are time normalised between ipsilateral limb impact events

4.2 | Electromyographic activity of the longissimus and adaptations during iFL and iHL

Longissimus is the largest equine epaxial muscle. Based on its anatomical location and attachments, it is thought to extend the spine when activated bilaterally in a concentric contraction, whereas unilateral concentric activation results in lateral bending and/or axial rotation.¹⁶ Here, longissimus had a bilateral, biphasic activation pattern in each stride cycle, with each burst corresponding to the second half of HL stance, where thoracolumbar flexion occurs (Figures 1 and 5). This biphasic pattern is well-documented in sEMG studies of quadrupedal trot on a treadmill,^{16,35–38} with longissimus function generally attributed to eccentric activity that stabilises the thoracolumbar spine during passive flexion.^{37–42} Across these studies, there are both interindividual variation in activation timing^{37,40,43} and variations in the number of activation bursts.^{41,43,44} Our findings support interindividual variation of longissimus activation, with some horses showing additional activation events in the first half of HL stance, producing additional bursts or elongation of the bi-phasic pattern. Von Scheven⁴⁴ explicitly described these additional bursts of longissimus activity in some horses during treadmill trot and, in the current study, they preceded peak thoracolumbar extension at approximately HL mid-stance (Figures 1 and 5). This is the first known study to acquire sEMG data from longissimus during overground quadrupedal trot on a hard surface, which is an important consideration given the known effect of both treadmill and surface type on locomotion, loading patterns, and workload.^{31,32,45} Indeed, loading experiments to alter locomotor forces acting on the trunk and hindlimbs of dogs, have noted adaptations in longissimus activation.^{41,42} Therefore, overground

locomotion on a hard-surfaced runway, as studied here, may yield different longissimus activation patterns. However, further research comparing muscle function during overground vs. treadmill locomotion and examination of antagonist muscles (eg, rectus abdominus) is required to confirm this.

Bilateral, significant increases in ARV observed at T14 and L1 during iHL support the theory posed by Fischer et al.⁴⁶ that bilateral adaptations in longissimus activity represent a stabilising function against compensatory sagittal plane forces during iHL, namely reduced vertical acceleration and displacement of the centre of mass during LS stance and vice versa during NLS stance.¹³ Supporting this, observational analysis of Figures 5 and 6 depicts increases in sEMG amplitude during iHL that are most pronounced in longissimus activation bursts during the first half of HL stance, where significant adaptations in thoracolumbar extension occurred, albeit to varying degrees between horses, because of documented adaptations in vertical forces acting on the trunk.¹³ These findings contrast with a study¹⁵ reporting significantly lower bilateral longissimus amplitude in horses with chronic, unilateral HL lameness, which was interpreted as a ‘more distinct resting phase’ between muscular activation bursts. Contrasting differences in longissimus activity could be related to chronicity of existing HL lameness compared with the acute, induced lameness evaluated in our study, but further comparative research is required to confirm this.¹⁵ Interestingly, nonsignificant changes in sEMG amplitude were also reported by Fischer et al.⁴⁶ for the LS and NLS of longissimus activity at L3/L4 sites in dogs with unilateral iHL during treadmill trot. Again, methodological differences make direct comparisons between studies difficult, particularly in relation to the type of locomotion (treadmill vs. overground),

sEMG processing and analysis methods,^{15,47} and lameness studied (acute/induced vs. chronic cases).¹⁵

Longissimus activation is affected by vertical and horizontal components of HL pro-retractor muscles.⁴² Temporal adaptations in HL pro-retraction have been described during iHL,⁴⁷ and in accordance with these changes, significantly delayed NLS longissimus activation timings were observed in our study and in Fischer et al.,⁴⁶ who also reported a nonsignificant trend for earlier activation on the LS, which was largely significant in our study. Trunk rotation towards the NLS has been described during iHL^{11,13} as a means to unload the LS HL.¹³ Significant changes in discrete lateral bending angles and continuous pelvic ROM data (Figure 3D,E), indicate that this compensatory mechanism was also observed in the current study. Lateral bending towards the NLS and pelvis roll and yaw rotations towards the LS were also found in this study, with significant differences in the SPM results for pelvic roll during LS stance (Figure 3D). It has been suggested that compensatory longitudinal rotations of the back and pelvis during iHL are driven by increased activity of NLS epaxial, as well as HL protractor muscles.⁴⁶ The significant increases in NLS longissimus amplitude observed in this study, as well as NLS superficial gluteal, biceps femoris and semitendinosus observed in St. George et al.¹⁶ support the realisation of increased lateral bending of the back towards the NLS and of the pelvis towards the LS. Taken together, these findings are the first to support postulated muscular adaptations for known compensatory weightbearing and movement patterns of the limbs, back, and pelvis during hindlimb lameness.

To our knowledge, this is the first study to examine equine muscle function during forelimb lameness. In contrast to iHL, longissimus amplitude and activation patterns at the sites evaluated remained largely unaltered during iFL, except for recordings at the LS L1 site, which significantly increased in amplitude (Figure 1). This finding appears to support the suggestion by Gómez-Álvarez et al.¹⁰: that increased activation of longissimus lumborum occurs during lame diagonal stance to produce lateral bending towards the LS in an attempt to shift the centre of mass towards the NLS in the horizontal plane.⁴⁸ It is possible that the pronounced increases in LS L1 activity reflect an active contraction to aid lateral bending towards the LS. However, interindividual differences in L1 activation were apparent in this study, further supporting the finding that horses adapt to iFL using individual compensatory movement patterns. Interestingly, significant changes were not observed in the thoracic recording sites, which were hypothesised to exhibit the greatest change during iFL, due to their closer proximity to the well-described compensatory 'head-nod'.¹³ It is possible that the 'head nod' produces subtle changes in thoracolumbar flexion/extension, but not enough to necessitate increased muscle activation of the longissimus at this region.

4.3 | Clinical relevance and further considerations

The lameness induction model was considered ideal for this preliminary research, as it produces a highly reliable and standardised condition for

study, but indeed lameness encountered clinically is variable and often chronic in nature. Furthermore, interindividual variation in the dataset from a small sample could be considered a limiting factor, but we argue that this finding reflects challenges within the clinical world, as well as previous research.^{6,8,34} Prior to this study, only clinical perceptions about adaptations in epaxial muscle activation during equine lameness existed. Although findings from this study offer the first objective data on underlying muscular adaptations in the equine back during lameness, clinical extrapolation of preliminary data is challenging. Thus, further studies employing a larger sample of clinical lameness cases are required. Nevertheless, it is clear from our results that adaptation mechanisms to lameness are complex and single limb lameness can affect kinematic and muscle activation of the back in an acute lameness model.⁴⁹

The known effect of speed on kinematic³⁷ and sEMG variables,⁵⁰ was addressed in this study by presenting results from models with and without a statistical correction for speed. This is especially relevant, as significant changes in stride velocity during equine lameness are known.⁴⁷ Therefore, it is only the adaptations in speed-corrected variables (Tables 1 and S2) that can be considered clinically relevant, as they are not confounded by the effects of speed and are thus the result of induced lameness. Finally, fewer group-averaged variables were found to be significantly altered during lameness conditions when analysed using SPM compared with linear mixed models. This discrepancy between the analysis of discrete and time series variables agrees with previous studies of equine biomechanics data.^{27,28,30} As alluded to in previous studies, this is because alpha is more tightly controlled when using SPM and the known variation in equine biomechanics data affects the level of significance using SPM.^{28,30} Based on this, Smit et al.²⁸ and Hobbs et al.³⁰ suggest that reaching significance may not be as important when using SPM to evaluate clinical implications and that data from individual horses should be assessed to ensure that subtle changes are not overlooked when considering group-level data. Our findings agree with this, as the clusters of data points that reached significance following SPM post hoc analysis of within-horse sEMG data (Figures S3 and S4), were often in accordance with the significant increases in discrete ARV and activation onset/offset variables (Tables 1 and S2), suggesting that time series data from individual horses should be evaluated when clinically assessing the effects of equine lameness.

5 | CONCLUSION

Distinctive differences in thoracolumbar and pelvic motion and underlying longissimus activity occur during iFL and iHL and have been measured here for the first time using combined motion capture and sEMG. iFL was characterised by significant decreases in peak thoracolumbar flexion angle, significant increases in pelvis pitching ROM, and significant changes in sEMG amplitude at L1 sites. In contrast, iHL was characterised by several significant adaptations including increases in thoracolumbar lateral bending towards the NLS and decreases towards the LS, decreased peak thoracolumbar flexion and increased peak extension angles, and increased pelvis yaw and

pitching ROM. These kinematic changes during iHL occurred alongside significant bilateral increases in longissimus activity and clear phasic shifts in activation timings. These findings suggest that, during iFL, thoracolumbar and pelvic movement adaptations occur primarily in the cranio-caudal direction, but this seemingly does not necessitate significant adaptations in longissimus activation at the thoracic regions studied here. Instead, significant changes in longissimus activation at the lumbar regions were observed during iFL, but this was largely horse-specific and may reflect another compensatory mechanism of increasing LS lateral bending to horizontally shift the centre of mass away from the affected limb. Whereas findings suggest that compensation for iHL primarily involves lateral bending and axial rotation to shift the centre of mass horizontally, and that these adaptations are facilitated by significant phasic shifts and increases in longissimus activation at both of the thoracic and lumbar regions studied here. The subtle and often horse-specific nature of these adaptations drives home the importance of future research to determine whether the significant changes observed here constitute clinically meaningful changes and to develop further objective clinical evaluation techniques for the equine back. These future studies are particularly important because many of the kinematic adaptations, and certainly the underlying neuromuscular adaptations, to lameness, as observed here, are undetectable through human observation alone.

AUTHOR CONTRIBUTIONS

Tijn J. P. Spoormakers, Lindsay St. George, Sarah Jane Hobbs and Filipe Manuel Serra Bragança contributed to conception and design of the study. Tijn J. P. Spoormakers, Lindsay St. George and Filipe Manuel Serra Bragança executed the study and collected data. Lindsay St. George and Filipe Manuel Serra Bragança conducted data processing and analysis. Filipe Manuel Serra Bragança and Ineke H. Smit performed the statistical analysis. Tijn J. P. Spoormakers and Lindsay St. George wrote the first draft of the manuscript. Filipe Manuel Serra Bragança and Ineke H. Smit wrote sections of the manuscript. All authors contributed to manuscript revision, read, and approved the submitted version, and confirm that all had access to the full dataset and take responsibility for the integrity of the data and the accuracy of data analysis. The authors want to acknowledge Suzan Büchli BSc, who assisted with the preparation and execution of the study.

ACKNOWLEDGEMENTS

The authors want to acknowledge Suzan Büchli BSc, who assisted with the preparation and execution of the study.

FUNDING INFORMATION

Morris Animal Foundation (Grant ID: D21EQ-406) and the British Society of Animal Science (BSAS) 2018 Steve Bishop Early Career Award.

CONFLICT OF INTEREST

Author Serge H. Roy is employed by Delsys Inc., the manufacturers of the sEMG sensors used in this study.

PEER REVIEW

The peer review history for this article is available at <https://publons.com/publon/10.1111/evj.13906>.

DATA AVAILABILITY STATEMENT

The data that support the findings of this study are available from the corresponding author upon reasonable request.

ETHICAL ANIMAL RESEARCH

Ethical approval for this study was obtained from Utrecht University (CCD: AVD108002015307) and the University of Central Lancashire (RE/17/08a_b).

ORCID

Tijn J. P. Spoormakers  <https://orcid.org/0000-0001-5093-0458>
 Lindsay St. George  <https://orcid.org/0000-0002-5531-1207>
 Sarah Jane Hobbs  <https://orcid.org/0000-0002-1552-8647>
 Hilary M. Clayton  <https://orcid.org/0000-0002-8759-0925>
 James Richards  <https://orcid.org/0000-0002-4004-3115>
 Filipe Manuel Serra Bragança  <https://orcid.org/0000-0001-8514-7949>

REFERENCES

- Landman MAAM, De Blaauw JA, van Weeren PR, Hofland LJ. Field study of the prevalence of lameness in horses with back problems. *Vet Rec.* 2004;155:165–8.
- Nielsen TD, Dean RS, Robinson NJ, Massey A, Brennan ML. Survey of the UK veterinary profession: common species and conditions nominated by veterinarians in practice. *Vet Rec.* 2014;174:324.
- Hausler KK. Chiropractic evaluation and management of musculoskeletal disorders. In: Ross MW, Dyson SJ, editors. *Diagnosis and Management of Lameness in the horse*. 2nd ed. St. Louis: Elsevier Inc.; 2011. p. 892–901.
- Jeffcott LB. Disorders of the thoracolumbar spine of the horse—a survey of 443 cases. *Equine Vet J.* 1980;12:197–210.
- Burns G, Dart A, Jeffcott LB. Clinical progress in the diagnosis of thoracolumbar problems in horses. *Equine Vet Educ.* 2018;30:477–85.
- Hardeman AM, Byström A, Roepstorff L, Swagemakers JH, van Weeren PR, Serra Bragança FM. Range of motion and between-measurement variation of spinal kinematics in sound horses at trot on the straight line and on the lunge. *PLoS One.* 2020;15(2):e0222822. <https://doi.org/10.1371/journal.pone.0222822>
- Faber M, Schamhardt H, van Weeren PR, Johnston C, Roepstorff L, Barneveld A. Basic three-dimensional kinematics of the vertebral column of horses walking on a treadmill. *Am J Vet Res.* 2000;61:399–406.
- Faber M, Johnston C, Schamhardt H, van Weeren PR, Roepstorff L, Barneveld A. Basic three-dimensional kinematics of the vertebral column of horses trotting on a treadmill. *Am J Vet Res.* 2001;62:757–64.
- Faber M, Johnston C, Schamhardt H, van Weeren PR, Roepstorff L, Barneveld A. Three-dimensional kinematics of the equine spine during canter. *Equine Vet J.* 2001;33:145–9.
- Gómez-Álvarez CB, Wennerstrand J, Bobbert MF, Lamers L, Johnston C, Back W, et al. The effect of induced forelimb lameness on thoracolumbar kinematics during treadmill locomotion. *Equine Vet J.* 2007;39:197–201.
- Gómez-Álvarez CB, Bobbert MF, Lamers L, Johnston C, Back W, van Weeren PR. The effect of induced hindlimb lameness on


- thoracolumbar kinematics during treadmill locomotion. *Equine Vet J.* 2008;40:147–52.
12. Wennerstrand J, Gómez Álvarez CB, Meulenbelt R, Johnston C, van Weeren PR, Roethlisberger-Holm K, et al. Spinal kinematics in horses with induced back pain. *Vet Comp Orthop Traumatol.* 2009;22:448–54.
 13. Buchner HHF, Savelberg HHCM, Schamhardt HC, Barneveld A. Head and trunk movement adaptations in horses with experimentally induced fore- or hindlimb lameness. *Equine Vet J.* 1996;28:71–6.
 14. Basmajian JV, De Luca CJ. Description and analysis of the EMG signal. *Muscles alive: their functions revealed by electromyography.* 5th ed. Baltimore, MD: Williams & Wilkins; 1985. p. 65–100.
 15. Zaneb H, Kaufmann V, Stanek C, Peham C, Licka TF. Quantitative differences in activities of back and pelvic limb muscles during walking and trotting between chronically lame and nonlame horses. *Am J Vet Res.* 2009;70:1129–34.
 16. St. George LB, Spoormakers TJP, Smit IH, Hobbs SJ, Clayton HM, Roy SH, et al. Adaptations in equine appendicular muscle activity and movement occur during induced fore- and hindlimb lameness: an electromyographic and kinematic evaluation. *Front Vet Sci.* 2022;9:989522. <https://doi.org/10.3389/fvets.2022.989522>
 17. Wakeling JM, Ritruetchai P, Dalton S, Nankervis K. Segmental variation in the activity and function of the equine longissimus dorsi muscle during walk and trot. *Equine Comp Exerc Physiol.* 2007;4:95–103.
 18. Cram JR, Rommen D. Effects of skin preparation on data collected using an EMG muscle-scanning procedure. *Biofeedback Self Regul.* 1989;14:75–82.
 19. Clancy EA, Morin EL, Merletti R. Sampling, noise-reduction and amplitude estimation issues in surface electromyography. *J Electromyogr Kinesiol.* 2002;12:1–16. [https://doi.org/10.1016/S1050-6411\(01\)00033-5](https://doi.org/10.1016/S1050-6411(01)00033-5)
 20. Merkens HW, Schamhardt HC. Evaluation of equine locomotion during different degrees of experimentally induced lameness I: lameness model and quantification. *Equine Vet J.* 1988;20(S6):99–106.
 21. Roepstorff C, Dittmann MT, Arpagaus S, Serra Bragança FM, Hardeman AM, Persson-Sjodin E, et al. Reliable and clinically applicable gait event classification using upper body motion in walking and trotting horses. *J Biomech.* 2021;114:110146. <https://doi.org/10.1016/j.jbiomech.2020.110146>
 22. Serra Bragança FM, Roepstorff C, Rhodin M, Pfau T, van Weeren PR, Roepstorff L. Quantitative lameness assessment in the horse based on upper body movement symmetry: the effect of different filtering techniques on the quantification of motion symmetry. *Biomed Signal Process Control.* 2020;57:57. <https://doi.org/10.1016/j.bspc.2019.101674>
 23. Rhodin M, Persson-Sjodin E, Egenvall A, Serra Bragança FM, Pfau T, Roepstorff L, et al. Vertical movement symmetry of the withers in horses with induced forelimb and hindlimb lameness at trot. *Equine Vet J.* 2018;50:818–24.
 24. Hardeman AM, Serra Bragança FM, Swagemakers JH, van Weeren PR, Roepstorff L. Variation in gait parameters used for objective lameness assessment in sound horses at the trot on the straight line and the lunge. *Equine Vet J.* 2019;51:831–9.
 25. St. George L, Hobbs SJ, Richards J, Sinclair J, Holt D, Roy SH. The effect of cut-off frequency when high-pass filtering equine sEMG signals during locomotion. *J Electromyogr Kinesiol.* 2018;43:28–40.
 26. St. George L, Roy SH, Richards J, Sinclair J, Hobbs SJ. Surface EMG signal normalisation and filtering improves sensitivity of equine gait analysis. *Comp Exerc Physiol.* 2019;15:173–85.
 27. St. George L, Clayton HM, Sinclair J, Richards J, Roy SH, Hobbs SJ. Muscle function and kinematics during submaximal equine jumping: what can objective outcomes tell us about athletic performance indicators? *Animals.* 2021;11:414. <https://doi.org/10.3390/ani11020414>
 28. Smit IH, Hernlund E, Brommer H, van Weeren PR, Rhodin M, Serra Bragança FM. Continuous versus discrete data analysis for gait evaluation of horses with induced bilateral hindlimb lameness. *Equine Vet J.* 2022;54:626–33.
 29. Pataky TC, Robinson MA, Vanrenterghem J. Vector field statistical analysis of kinematic and force trajectories. *J Biomech.* 2013;46:2394–401.
 30. Hobbs SJ, Robinson MA, Clayton HM. A simple method of equine limb force vector analysis and its potential applications. *PeerJ.* 2018;6:e4399. <https://doi.org/10.7717/peerj.4399>
 31. Buchner HHF, Savelberg HHCM, Schamhardt HC, Merkens HW, Barneveld A. Kinematics of treadmill versus overground locomotion in horses. *Vet Q.* 1994;16:87–90.
 32. Gómez Álvarez CB, Rhodin M, Byström A, Back W, van Weeren PR. Back kinematics of healthy trotting horses during treadmill versus over ground locomotion. *Equine Vet J.* 2009;41:297–300.
 33. Pourcelot P, Audigié F, Degueurce C, Denoix JM, Geiger D. Kinematics of the equine back: a method to study the thoracolumbar flexion-extension movements at the trot. *Vet Res.* 1998;29:519–25.
 34. Byström A, Hardeman AM, Serra Bragança FM, Roepstorff L, Swagemakers JH, van Weeren PR, et al. Differences in equine spinal kinematics between straight line and circle in trot. *Sci Rep.* 2021;11:12832. <https://doi.org/10.1038/341598-021-92272-2>
 35. Robert C, Audigié F, Valette JP, Pourcelot P, Denoix JM. Effects of treadmill speed on the mechanics of the back in the trotting saddlehorse. *Equine Vet J.* 2001;33(S33):154–9.
 36. Robert C, Valette JP, Denoix JM. The effects of treadmill inclination and speed on the activity of two hindlimb muscles in trotting horse. *Equine Vet J.* 2000;32:312–7.
 37. Robert C, Valette JP, Pourcelot P, Audigié F, Denoix JM. Effects of trotting speed on muscle activity and kinematics in saddlehorses. *Equine Vet J.* 2002;34(S34):295–301.
 38. Licka T, Peham C, Frey A. Electromyographic activity of the longissimus dorsi muscles in horses during trotting on a treadmill. *Am J Vet Res.* 2004;65:155–8.
 39. Kienapfel K, Preuschoft H, Wulf A, Wagner H. The biomechanical construction of the horse's body and activity patterns of three important muscles of the trunk in the walk, trot and canter. *J Anim Physiol Anim Nutr.* 2018;102:e818–27. <https://doi.org/10.1111/jpn.12840>
 40. Robert C, Valette JP, Denoix JM. The effects of treadmill inclination and speed on the activity of three trunk muscles in the trotting horse. *Equine Vet J.* 2001;33:466–72.
 41. Ritter DA, Nassar PN, Fife M, Carrier DR. Epaxial muscle function in trotting dogs. *J Exp Biol.* 2001;204:3053–64.
 42. Schilling N, Carrier DR. Function of the epaxial muscles during trotting. *J Exp Biol.* 2009;212:1053–63.
 43. Vögele AM, Zsoldos RR, Krüger B, Licka T. Novel methods for surface emg analysis and exploration based on multi-modal Gaussian mixture models. *PLoS One.* 2016;11(6):e0157239. <https://doi.org/10.1371/journal.pone.0157239>
 44. Von Scheven C. *The anatomy and function of the equine thoracolumbar Longissimus dorsi muscle* [thesis]; 2010:<https://doi.org/10.5282/edoc.12178>
 45. Crevier-Denoix N, Ravary-Plumioën B, Vergari C, Camus M, Holden-Douilly L, Falala S, et al. Comparison of superficial digital flexor tendon loading on asphalt and sand in horses at the walk and trot. *Vet J.* 2013;198:e130–6. <https://doi.org/10.1016/j.tvjl.2013.09.047>
 46. Fischer S, Nolte I, Schilling N. Adaptations in muscle activity to induced, short-term hindlimb lameness in trotting dogs. *PLoS One.* 2013;8(11):e80987. <https://doi.org/10.1371/journal.pone.0080987>
 47. Buchner HHF, Savelberg HHCM, Schamhardt HC, Barneveld A. Limb movement adaptations in horses with experimentally induced fore-or hindlimb lameness. *Equine Vet J.* 1996;28:63–70.
 48. Buchner HHF, Obermüller S, Scheidl M. Body centre of mass movement in the lame horse. *Equine Vet J.* 2001;33:122–7.
 49. Weishaupt MA, Wiestner T, Hogg HP, Jordan P, Auer JA. Compensatory load redistribution of horses with induced weight-bearing forelimb lameness trotting on a treadmill. *Vet J.* 2006;171:135–46.

50. Hof AL, Elzinga H, Grimmer W, Halbertsma JPK. Speed dependence of averaged EMG profiles in walking. *Gait Posture*. 2002; 16:78–86.

SUPPORTING INFORMATION

Additional supporting information can be found online in the Supporting Information section at the end of this article.

How to cite this article: Spoormakers TJP, St. George L, Smit IH, Hobbs SJ, Brommer H, Clayton HM, et al. Adaptations in equine axial movement and muscle activity occur during induced fore- and hindlimb lameness: A kinematic and electromyographic evaluation during in-hand trot. *Equine Vet J*. 2023;55(6):1112–27. <https://doi.org/10.1111/evj.13906>



LOOKING AT YOUR PRACTICE THROUGH A DIFFERENT LENS

Speak to your MSD Equine Account Manager today to find out more about our **innovative practice support solutions.**

MSD Animal Health UK Limited. Registered office Walton Manor, Walton, Milton Keynes MK7 7AJ, UK. Registered in England & Wales no. 946942. www.msd-animal-health.co.uk
Copyright © 2021 MSD Animal Health UK Limited. All rights reserved.
UK-EQU-211000005 10/21

 **MSD**
Animal Health